JOURNAL OF PROPULSION AND POWER
Vol. 27, No. 1, January–February 2011

# Improved Modal Localization and Excitation Factors for Understanding Mistuned Bladed Disk Response

Jianyao Yao,* Jianjun Wang,† and Qihan Li‡
*Beijing University of Aeronautics and Astronautics, 100191 Beijing, People's Republic of China*

DOI: 10.2514/1.48244

**The nodal diameter spectrum is defined based on the discrete Fourier transform of the mode shapes of bladed disks. The dynamic characteristics analysis and assessment for a simplified bladed disk is performed using the concept of the nodal diameter spectrum. For free vibration, the mode localization factor is defined based on the nodal diameter spectrum, and the probabilistic modal properties are obtained for the bladed disk with random mistuning of blade stiffness. For the forced vibration, the modal excitation factor is defined based on the nodal diameter spectrum to evaluate the similarity of engine-order excitation and the mistuned modes. The threshold phenomenon of random mistuning strength and the existence of optimal intentional mistuning are well explained through the combined effects of the modal excitation factor and the corresponding mode localization level of the mistuned mode shape on the response amplitude magnification. The numerical results indicate that the nodal diameter spectrum is an important parameter describing the spatial distributions of the mistuned mode shapes and could be widely applied in the analysis of the dynamic characteristics of mistuned bladed disks.**

## I. Introduction

DUE to the small imperfections in manufacturing, assembly process, and uneven wear, blade mistuning is inevitable in practical bladed disks. The dynamic characteristics of mistuned bladed disks have been extensively investigated in recent decades [1,2]. Many research results indicate that the stress levels and vibration amplitude distributions of mistuned bladed disks are highly sensitive to mistuning variations even in the small ranges restricted by manufacturing tolerance. It is therefore of great interest to study the dynamic characteristics of mistuned bladed disks to predict and control the adverse influence of random mistuning.

Two main dynamic characteristics of mistuned bladed disks are mode localization (free vibration) and vibration amplitude magnification (forced vibration). For the free vibration, the mode localization factor (MLF) is used to evaluate the difference between the mistuned mode and the corresponding tuned mode. Wang et al. [3,4] defined three kinds of MLFs based on the modal displacement, modal stress, and modal strain energy. These MLFs have clear physical concepts and could quantify the level of localization of mistuned modes. The main deficiency of these MLFs is that the tuned and mistuned modes' pair is chosen by the same frequency order rather than the resemblance between the modes. To improve the description of the MLF, we give the definition of the nodal diameter spectrum (NDS) based on the discrete Fourier transform (DFT) of mode shapes, and we correlate the mistuned mode with the tuned mode that has the largest ratio of this mistuned mode. Castanier and Pierre [5] first used DFT as the basis to evaluate the mistuned modes, but they only gave the preliminary explanation of the physical mechanism of mistuning. More recently, Klauke et al. [6] proposed the definitions of the mode fill factor and localization factor based on the concept of DFT to evaluate the free vibration characteristics of mistuned bladed disks. In this paper, we give a more simple and clear definition of MLF based on the NDS of mode shapes, which will be introduced in detail in Sec. II.

For the forced vibration, amplitude magnification is always used to assess the effects of mistuning. Several studies have demonstrated that the amplitude magnification tends to exhibit a peak value with respect to mistuning strength [7–9]. That is, the maximum forced response increases with increased mistuning up to a certain level, but a further increase in mistuning actually results in lower forced amplitudes. This remarkable effect could be named the threshold phenomenon. Researchers also found that some appropriate intentional mistuning can alleviate the adverse influence of random mistuning on the forced response of mistuned bladed disks [5,7,8]. Although these effects of random and intentional mistuning are studied extensively, their physical mechanisms remain unclear. Ottarsson and Pierre [10] and Castanier and Pierre [5] gave the primary explanations of the mistuning mechanism using the mass-spring model. The results indicate that the intentional mistuning makes the rotor less susceptible to being strongly excited by engine-order (EO) excitation by spreading out the nodal diameter content of the modes. Here, the influence of the type and strength of intentional mistuning on amplitude magnification will be explained using the concept of the modal excitation factor (MEF) and the MLF.

This paper is organized as follows. We first give the mathematical definition of NDS and explain its physical meaning in Sec. II. In Secs. III and IV, the effects of random and intentional mistuning on NDS are investigated, and the threshold phenomenon is explained in view of the concepts of NDS and MEF; the mechanisms of intentional mistuning and the combined effects of intentional and random mistuning on the forced response are also illustrated. In the last section, conclusions from this study are summarized.

## II. Definition of Nodal Diameter Spectrum and its Applications

### A. Definition of Nodal Diameter Spectrum

The modes of tuned bladed disks can be written in complex, traveling wave form [11,12]. When the tuned system modes are expressed in this manner, the amplitudes of every blade in a mode are the same, but each blade has a different phase. That means, in the standing wave form, the tuned mode shapes are extended in the circumferential direction in harmonic form. Therefore, the modal displacements of every node with exact the same position of the sector (for example, the blade tip) can be written as

Received 23 November 2009; revision received 24 August 2010; accepted for publication 17 September 2010. 

*Ph.D. Candidate, 405 Laboratory of the School of Jet Propulsion; yaojianyao@sjp.buaa.edu.cn.

†Professor, 405 Laboratory of the School of Jet Propulsion; wangjjb@263.net (Corresponding Author).

‡Professor, 405 Laboratory of the School of Jet Propulsion; liqihan@buaa.edu.cn.

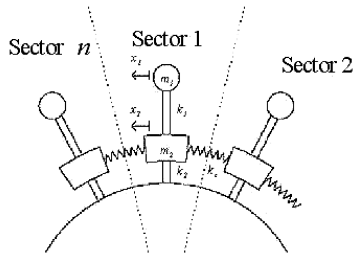


**Fig. 1 Bladed disk model.**

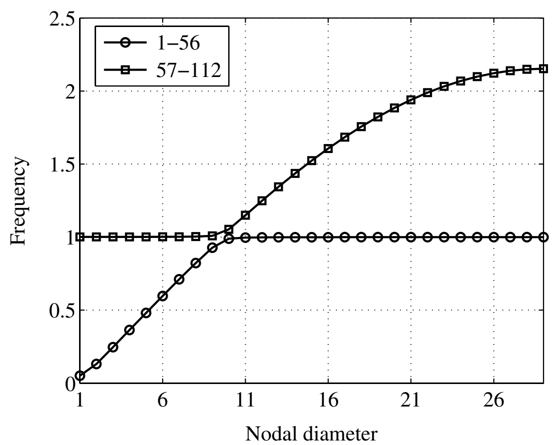


**Fig. 2 Nodal diameter-frequency map.**

$$X_i = X \cos\left(\frac{2\pi S}{N} i\right) \tag{1}$$

where $X$ is the harmonic amplitude, $S$ is the nodal diameter number, $N$ is the number of blades (or sectors), and $i$ is the blade index. The vector $\Phi = \{X_1 \quad \cdots \quad X_N\}^T$ represents the spatial distribution of the mode shape, and we name it the representative subeigenvector. If we perform DFT on vector $\Phi$, the harmonic component is nonzero only in diameter $S$.

If the tuned bladed disk has $N_A$ DOFs, the $N_A$ linear-independent eigenvectors form a complete set of basis vectors of the $N_A$-dimensional linear vector space $V$. Every $v \in V$ can be written as the linear combination of these basis vectors. Therefore, the mistuned mode shapes can also be expressed as the linear combination of tuned shapes. In practice, we cannot and need not obtain all $N_A$ eigenvectors, since $N_A$ is too large. Instead, we only compute the first several eigenvalues and corresponding eigenvectors of interest. For the bladed disk, the mode shapes are clustered and may be fairly well isolated if the disk is relatively stiff. These modes, with closely spaced frequencies and the same blade vibration type (e.g., bending) but corresponding to different numbers of nodal diameters in the disk, are often referred to as a family of modes. So, when describing the mistuned modes, we can only use several families (subset of nominal system [11]) or even a family (fundamental model of mistuning [12]) of tuned modes to approximate the complete basis.

For the subeigenvectors in Eq. (1), it is a subset of the full mode shapes. In a mode family including $N$ mode shapes, the $N$ tuned subeigenvectors also form a complete basis of $N$-dimensional vector space. Therefore, the mistuned subeigenvector $\Phi_m$ can be expressed as the linear combination of the tuned subeigenvectors:

$$\Phi_m = \sum_{i=1}^{N} a_i \Phi_i \tag{2}$$

where $\Phi_i$ is the tuned subeigenvector in harmonic form as Eq. (1). Performing DFT on $\Phi_m$, we can obtain the nodal diameter components of the mistuned mode shape,

$$y = \frac{1}{N} F \Phi_m \tag{3}$$

where $F$ is a Vandermonde matrix:

$$F = \begin{bmatrix} e^{(2\pi i/N)0\cdot 0} & e^{(2\pi i/N)0\cdot 1} & \cdots & e^{(2\pi i/N)0\cdot(N-1)} \\ e^{(2\pi i/N)1\cdot 0} & e^{(2\pi i/N)1\cdot 1} & \cdots & e^{(2\pi i/N)1\cdot(N-1)} \\ \vdots & \vdots & \ddots & \vdots \\ e^{(2\pi i/N)(N-1)\cdot 0} & e^{(2\pi i/N)(N-1)\cdot 1} & \cdots & e^{(2\pi i/N)(N-1)\cdot(N-1)} \end{bmatrix} \tag{4}$$

According to the properties of matrix $F$, when $k_1 + k_2 = N + 2$, we have

$$y(k_1) = y(k_2)' \tag{5}$$

Therefore, we only need the first half of $y$, and this is the reason that the highest nodal diameter of an$N$-sector bladed disk is $[N/2]$, where $[\cdot]$ denotes the integer part. To make entries of $y$ equal to the harmonic amplitude in Eq. (1), we should scale them appropriately and define them as the NDS $\phi_{\mathrm{ND}}$. When $N$ is odd,

$$\phi_{\mathrm{ND}}(1) = \mathrm{abs}[y(1)]$$
$$\phi_{\mathrm{ND}}\left(2\colon \frac{N-1}{2}\right) = \mathrm{abs}\left[y\left(2\colon \frac{N-1}{2}\right)\right] \times 2 \tag{6}$$

and when $N$ is even,

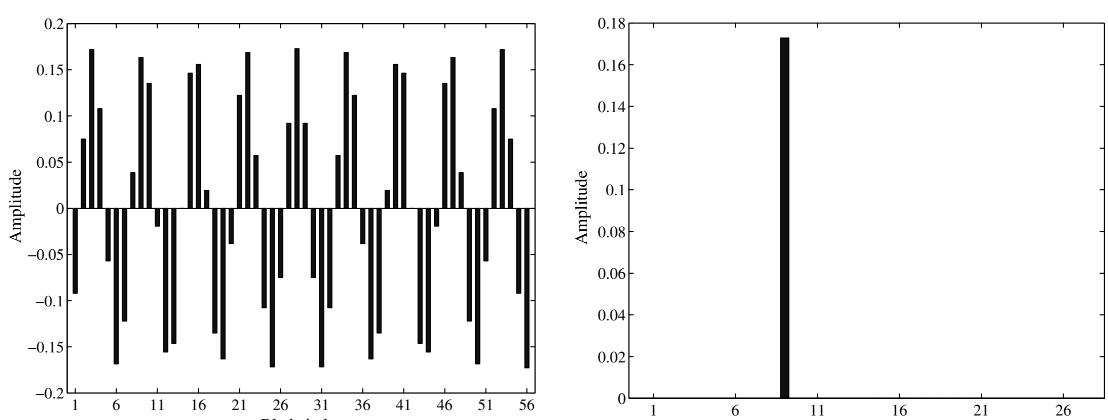


**a) Mode shape** **b) NDS**

**Fig. 3 The 18th-mode shapes and corresponding NDS of the tuned bladed disk.**

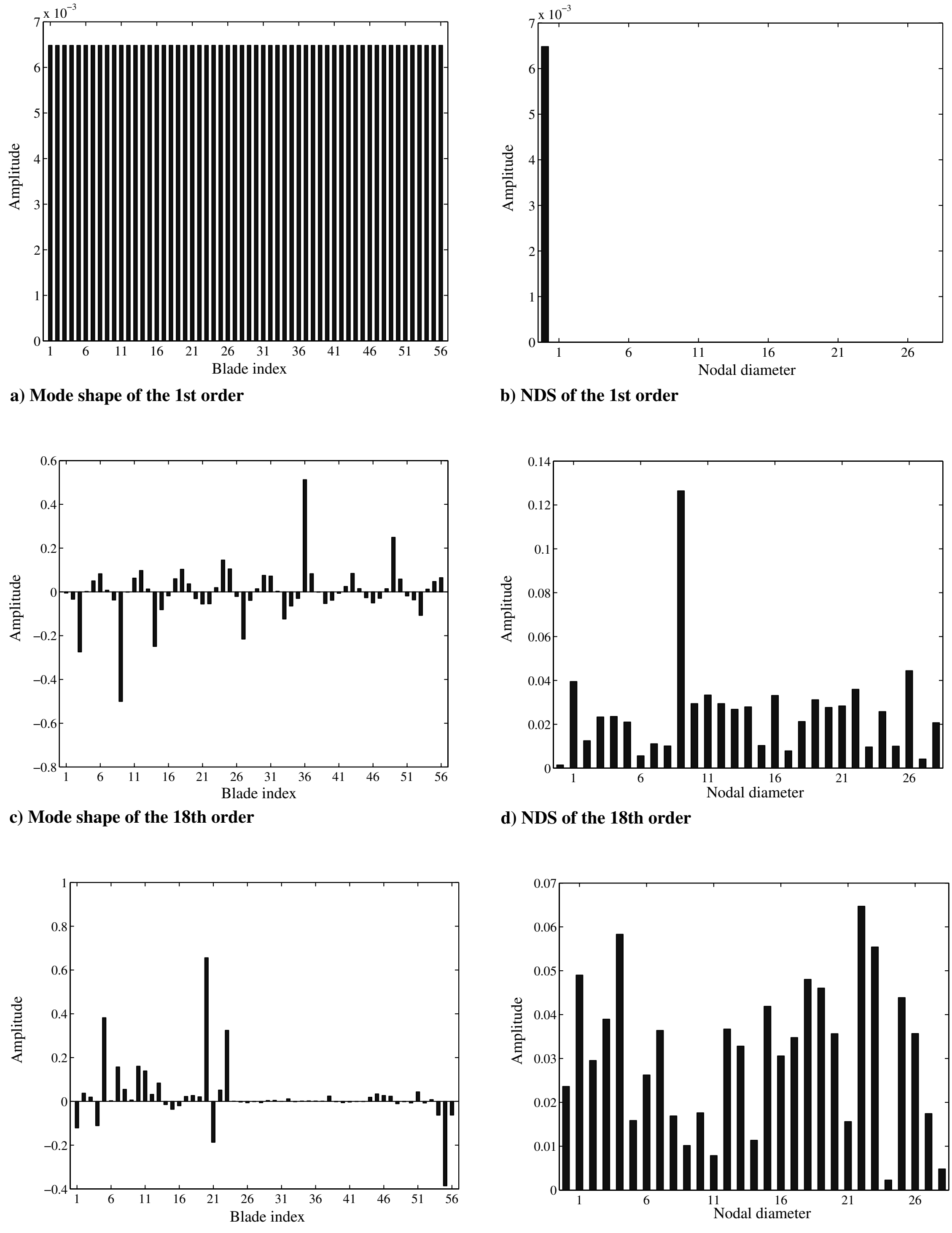


**a) Mode shape of the 1st order** **b) NDS of the 1st order**

**c) Mode shape of the 18th order** **d) NDS of the 18th order**

**e) Mode shape of the 56th order** **f) NDS of the 56th order**

**Fig. 4 The mode shapes and corresponding NDS of the mistuned bladed disk.**

$$\begin{gathered}\phi_{\mathrm{ND}}(1)=\mathrm{abs}[y(1)]\\ \phi_{\mathrm{ND}}\left(2\colon\ \frac{N}{2}-1\right)=\mathrm{abs}\left[y\left(2\colon\ \frac{N}{2}-1\right)\right]\times 2\\ \phi_{\mathrm{ND}}\left(\frac{N}{2}\right)=\mathrm{abs}\left[y\left(\frac{N}{2}\right)\right]\end{gathered}\tag{7}$$

NDS $\phi_{\mathrm{ND}}$ describes the ratios of different nodal diameter components (0 to $N/2$ or $(N-1)/2$) in the mistuned mode. The nodal diameter with a maximal ratio $\max(\phi_{\mathrm{ND}})$ is called the dominant nodal diameter of the mode shape.

### B. Definition of Mode Localization Factor

MLF is often used to describe the difference between the mistuned and tuned mode shapes. Wang et al. [3,4] gave the definition of MLF based on the nondimensional maximal displacement $u$ of the subeigenvector $\Phi$, and $u$ is defined as

$$u=\frac{\max[\mathrm{abs}(\Phi)]}{\mathrm{sum}[\mathrm{abs}(\Phi)]}\tag{8}$$

as $u$ gives the ratio of the maximal vibration amplitude and the sum of the vibration amplitudes of all sectors and, the larger $u$ is, the more severe the mode is localized in a single sector. For a pair of modes,

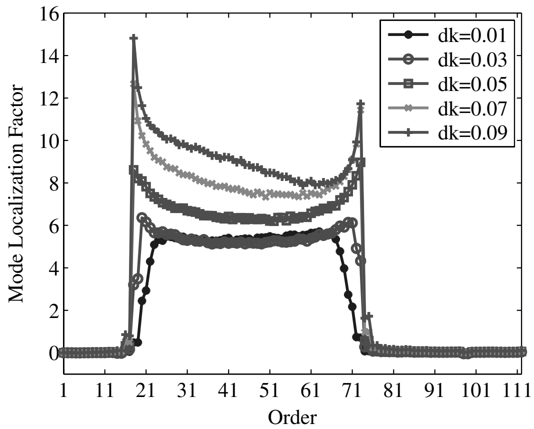


**Fig. 5 MLF with different random mistuning strengths.**

before and after the mistuning is introduced into the bladed disk, the MLF of a mistuned mode can be defined as

$$\mathrm{MLF} = \frac{u_m - u_n}{u_n} \tag{9}$$

where $u_m$ and $u_n$ are the dimensionless maximal displacements for the mistuned and corresponding tuned mode shape.

In [3,4], the pair of mistuned and tuned modes is chosen according to the frequency order; that is, the $i$th mistuned mode corresponds to the $i$th tuned mode. However, when mistuning is considered, the dominant nodal diameter of the mistuned modes may change arbitrarily; therefore, the physical meaning of the frequency-order corresponding principle may not be much clearer. Based on the concept of NDS, we improve the method of choosing the tuned mode corresponding to the mistuned one; that is, the tuned mode is determined by the dominant nodal diameter rather than by the natural frequency-order sequence, and it can be written as

$$\Phi_n = \{\cos(1\theta) \quad \cdots \quad \cos(N\theta)\}^T \tag{10}$$

where $\theta = 2\pi S/N$, and $S$ is the dominant nodal diameter of $\Phi_m$.

The definition of MLF in Eq. (9) has the three advantages. First, complex vibration behavior of the mistuned bladed disk can be evaluated using this simple illustrative indictor. Second, the MLF is directly connected to the modal displacement, and it can roughly reflect the localization of the modal response. Third, it is easy to compute and only need the information of the mistuned mode.

### C. Definition of Modal Excitation Factor

According to the requirement of the correlation of the vibration mode shape and the excitation mode shape, a $k$th nodal diameter mode can only be excited by a $k$th EO in the case of a tuned system. The EO excitation can be written as the traveling wave excitation; that is, the excitation on each sector has the same amplitude but a constant phase difference between the adjacent sector. Therefore, the excitation on the $i$th blade can be written as

$$f_i = F\sin(\omega t + i\theta_E) \tag{11}$$

where $E$ is the EO, and $\theta_E = 2\pi E/N$ is the excitation phase difference between adjacent sectors. Since the traveling wave excitation is a combination of pure sine and cosine functions, the modal excitation cannot be directly obtained from the dot product of the harmonic amplitude for the excitation and the mode shape vector.

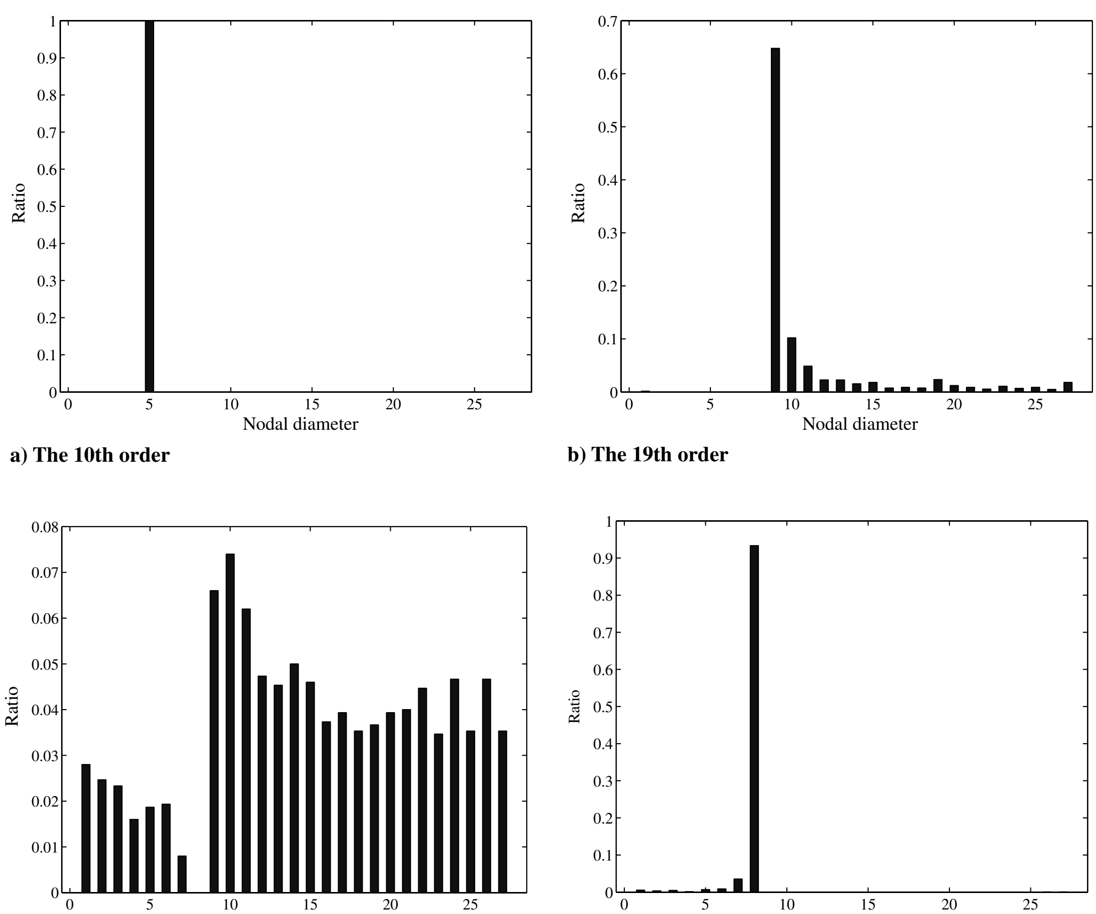


**a) The 10th order** **b) The 19th order**

**c) The 29th order** **d) The 73th order**

**Fig. 6 Histograms of the dominant nodal diameters for the mistuned mode shapes, with random mistuning strengths [−%5, %5].**

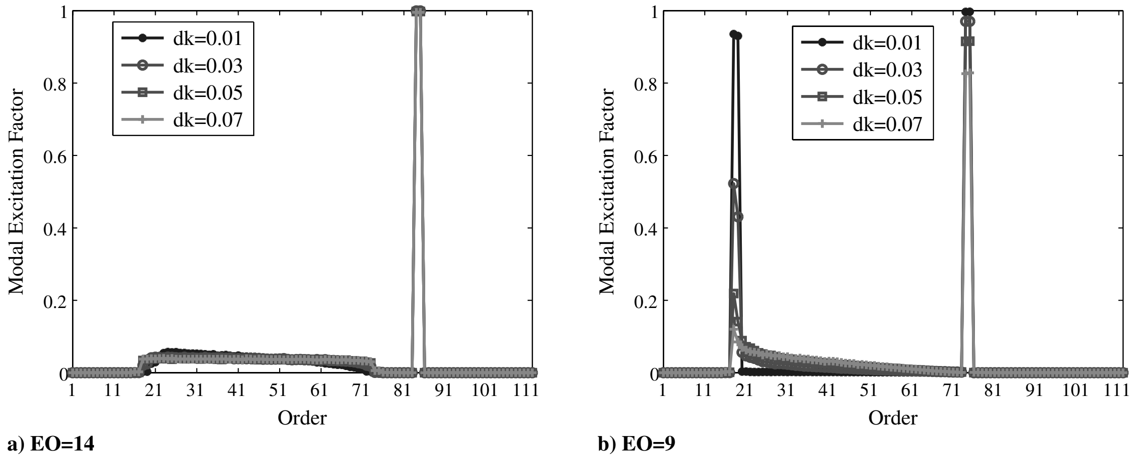


**Fig. 7 MEF with different strength of random mistuning.**

The real aerodynamic excitations that the industrial bladed disk are subjected to are much more complicated than Eq. (11), but they can still be generally expressed as the combination of traveling wave excitation with different EOs and amplitudes. The modal excitations for this situation are more difficult to obtain. Theoretically, the spatial distributions of these kinds of excitations at different times are the same but with phase difference. To describe the basic characteristics of the spatial distribution of the excitations, we can also use the concept of NDS to EO components of the excitation, and we define it as the NDS of the excitations. For the excitation as Eq. (11), as the tuned mode shape, the nonzero component of NDS only exists in $E$.

As mentioned in Sec. II.A, the mode shape of the mistuned bladed disk has more than one nodal diameter component; that is, there is more than one nonzero entry in $\Phi_{\mathrm{ND}}$. To describe the similarity between the NDS of the excitation and the mistuned mode shape, we define the MEF with the aid of the concept of modal assurance criterion,

$$\mathrm{MEF} = \frac{(\phi_{\mathrm{ND}n}^T \phi_{\mathrm{ND}m})^2}{(\phi_{\mathrm{ND}n}^T \phi_{\mathrm{ND}n})(\phi_{\mathrm{ND}m}^T \phi_{\mathrm{ND}m})} \tag{12}$$

where $\phi_{\mathrm{ND}n}$ is the NDS of excitation, and $\phi_{\mathrm{ND}m}$ is the NDS of the mistuned mode shape. MEF gives a coarse estimation of modal excitation. When $\mathrm{MEF} = 1$, the NDS of the excitation and the mode shape are perfectly the same, and the mode shape is fully excited; when $\mathrm{MEF} = 0$, the two NDS are orthogonal to each other, and the modal excitation is zero. In most cases, we have $0 < \mathrm{MEF} < 1$, the closer the MEF is to one, the more similar the excitation is to the mode shape and the more likely it will be that the mode shapes are excited by the given excitation.

## III. Nodal Diameter Spectrum and Mode Localization Factor of the Mode Shapes of the Bladed Disk

### A. Model of the Simplified Bladed Disk

To illustrate the application and effectiveness of the NDS in the assessment of dynamic characteristics for a mistuned bladed disk, we use a simplified bladed disk as the numerical example. The example used for the bladed disk is a mass-spring model with $N = 56$ sectors. There are two deg of freedom (DOFs) per sector: one DOF represents the blade motion and the other the disk motion. The nondimensional model parameters are as follows: $k_1 = 1$, $k_2 = 1.1$, $k_c = 493$, $m_1 = 1$, and $m_2 = 426$. The schema of the example of the bladed disk is shown in Fig. 1.

The dynamic characteristics of the preceding model for both tuned and mistuned cases were deeply discussed in [9,13]. Figure 2 shows the natural frequencies of the tuned bladed disk model. The results show that the modal density is considerably high, close to the blade-alone frequency $\sqrt{k_1/m_1} = 1$, and there are 56 (half of the total number) natural frequencies between 0.98 and 1.01. Notice that the natural frequencies veer at nodal diameters of eight and nine in the nodal diameter-frequency map, where the vibration localization phenomenon is most prone to appear. Since the vibration of disk DOFs are not sensitive to blade mistuning, we focus on the blade motion in blade-mistuned blade disks.

### B. Nodal Diameter Spectrum of Tuned Mode Shapes

The NDS of tuned mode shapes of blade DOFs can be obtained using Eq. (7), as is shown in Fig. 3. We can see that there is only one nonzero nodal diameter component for the tuned mode shape, and its

**Table 1 Mean of MLFs and MEFs of excited modes for $E = 14$**

| | MLFs | | | | MEFs | | | |
|---|---|---|---|---|---|---|---|---|
| Order | 28 | 29 | 84 | 85 | 28 | 29 | 84 | 85 |
| $dk = 0.01$ | 5.4060 | 5.3720 | 0.0170 | 0.0153 | 0.0546 | 0.0531 | 0.9999 | 0.9999 |
| $dk = 0.03$ | 5.5599 | 5.4225 | 0.0516 | 0.0462 | 0.0431 | 0.0406 | 0.9991 | 0.9991 |
| $dk = 0.05$ | 6.8054 | 6.8098 | 0.0869 | 0.0776 | 0.0389 | 0.0393 | 0.9976 | 0.9976 |
| $dk = 0.07$ | 9.6566 | 8.4731 | 0.1239 | 0.1104 | 0.0381 | 0.0375 | 0.9953 | 0.9953 |

**Table 2 Mean of MLFs and MEFs of excited modes for $E = 9$**

| | MLFs | | | | MEFs | | | |
|---|---|---|---|---|---|---|---|---|
| Order | 18 | 19 | 74 | 75 | 18 | 19 | 74 | 75 |
| $dk = 0.01$ | 0.4830 | 0.4874 | 0.0721 | 0.0766 | 0.9356 | 0.9302 | 0.9968 | 0.9968 |
| $dk = 0.03$ | 3.2014 | 3.4896 | 0.2762 | 0.2839 | 0.5226 | 0.4307 | 0.9704 | 0.9704 |
| $dk = 0.05$ | 8.6158 | 8.2091 | 0.5511 | 0.5710 | 0.2188 | 0.1414 | 0.9152 | 0.9159 |
| $dk = 0.07$ | 12.666 | 10.924 | 0.9670 | 0.9982 | 0.1204 | 0.0851 | 0.8260 | 0.8281 |

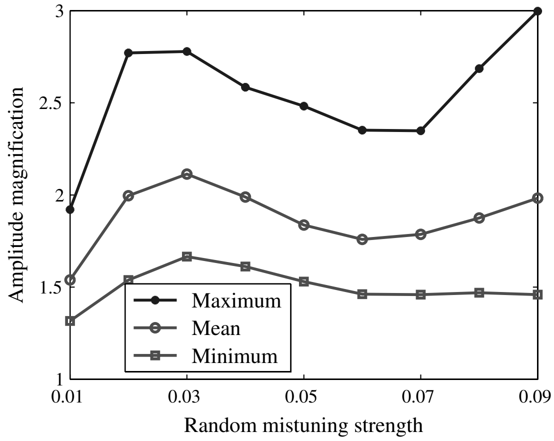


**Fig. 8 Amplitude magnification for different random mistuning strengths. The maximum and minimum are the maximal and minimal values obtained from Monte Carlo simulations of the 1500 samples. However, due to the finite sample number, the maximal amplitude magnification factors are less the Whitehead factor $(1 + \sqrt{56})/2$ [14], and the maximum and minimum are the extreme response values of the 1500 sample bladed disks.**

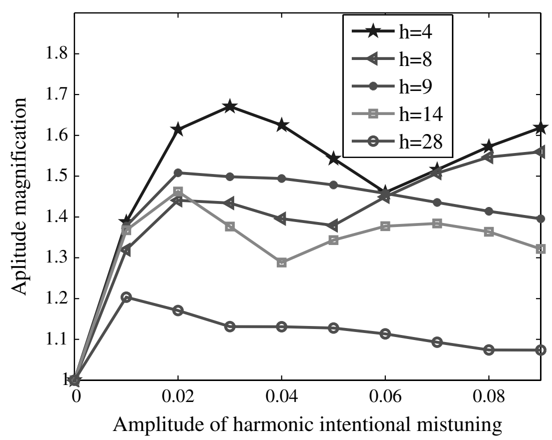


**Fig. 9 Amplitude magnification with different types of intentional mistuning.**

amplitude is equal to $X$ in Eq. (1), the harmonic amplitude of the mode shape.

### C. Nodal Diameter Spectrum of Mistuned Mode Shapes

For the mistuned bladed disk, there will be more than one nonzero entry in $\Phi_{\text{ND}}$ for the mode shapes. The sensitivities to mistuning for the blade- and disk-dominated vibrations are also different. Given a set of uniformly distributed random mistuning ([−3%, 3%], blade stiffness mistuning), the mode shapes and the corresponding NDS are shown in Fig. 4.

The results indicate that the blade-dominated vibrations are very sensitive to the given random mistuning, and the mode shapes and NDS are quite different from the corresponding tuned case, as shown in Figs. 4b and 4c. It is worth noting that, for the 18th order at the veering zone, the dominant nodal diameter is still nine, the same as the tuned case; for the 56th order, the NDS of the mistuned mode shape is extended evenly to almost all the nodal diameters. The disk-dominated vibration is much less sensitive to random mistuning, and the mistuned mode shape and NDS are almost the same as the tuned case, as shown in Fig. 4a.

### D. Mode Localization Factor of the Mistuned Mode Shapes

For the mistuned bladed disks, we always want to obtain the probabilistic dynamic characteristics. Therefore, the sampling process of random mistuning is needed. Here, four groups of the uniformly distributed blade mistuning of blade stiffness with different strengths are considered, and there are 1500 samples in each group. The mean of the calculated MLFs for every order (1–112) are shown in Fig. 5. According to the results, we can conclude the following:

1) The modes are highly localized in the blade-dominated vibrations, and MLFs increase monotonically with the increasing of random mistuning strength.

2) The most severe localization phenomena (maximal MLFs) take place at the adjacent orders of the blade- and disk-dominated vibrations, corresponding to the blade–disk coupled vibration: for example, the 18th and 73th orders.

3) The disk-dominated vibrations are not sensitive to blade mistuning, and the MLFs are almost zero at these orders.

### E. Distributions of Dominant Nodal Diameter

The dominant nodal diameter determines the mistuned mode shape and is the most susceptible to be excited by the traveling excitation, which has the same EO as the dominant nodal diameter. Using the third group of mistuning samples with $dk = 0.05$, in Sec. III.D, the histograms of dominant nodal diameters of a random mistuned bladed disk are shown in Fig. 6. There are three kinds of mistuned modes considered: the disk-dominated mode (the 10th order), the blade-dominated mode (the 29th order), and the coupled modes (the 19th and 73th orders). The results indicate the following:

1) Since the disk-dominated mode is not sensitive to mistuning, the introduced random mistuning does not change the distribution dominant nodal diameters, as shown in Fig. 6a.

2) The dominant nodal diameters of the blade-dominated mode spread out widely, as shown in Fig. 6c.

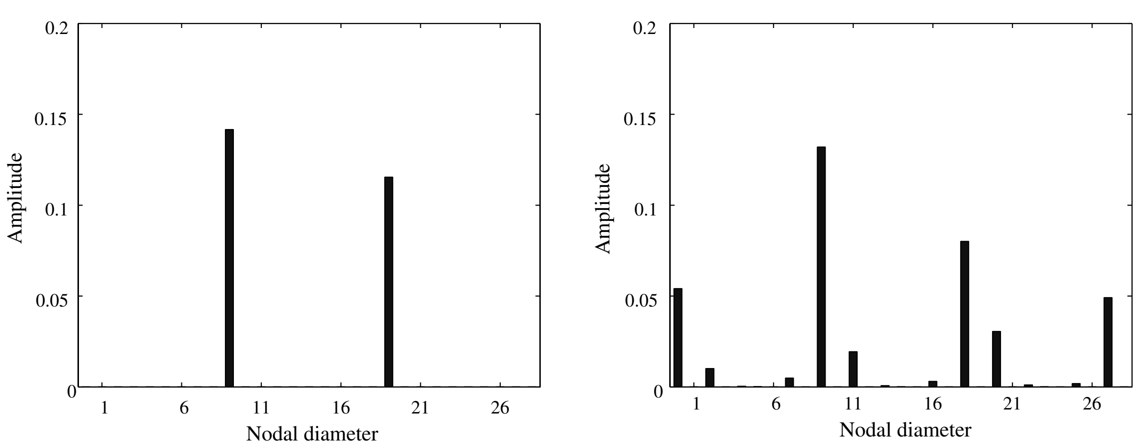


**a) $h = 28$, $A = 0.04$** **b) $h = 9$, $A = 0.04$**

**Fig. 10 NDS of 18th mode with intentional mistuning.**

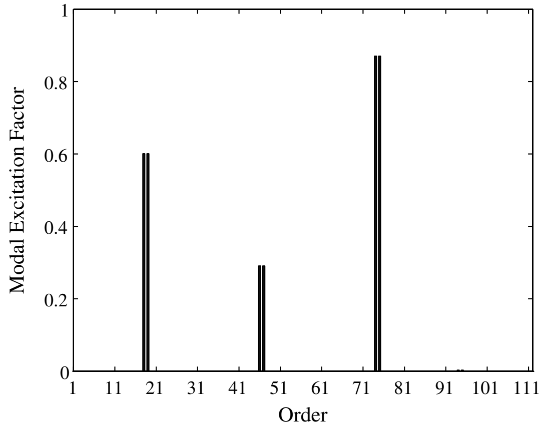

a) $h = 28, A = 0.04$

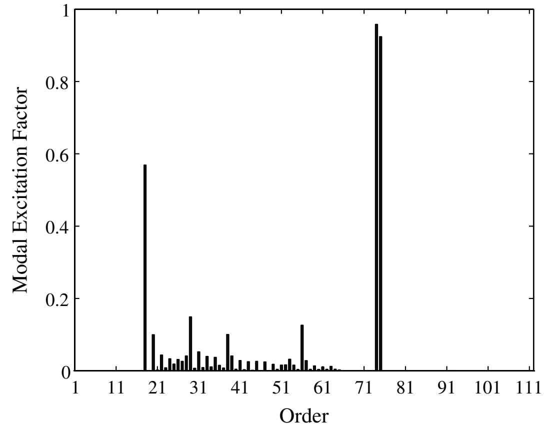

b) $h = 9, A = 0.04$

**Fig. 11 MEFs with intentional mistuning.**

3) For the coupled modes, the dominant nodal diameters mainly keep the same position as the tuned case, but they disperse slightly to the other nodal diameters, as shown in Figs. 6b and 6d.

## IV. Application of Mode Localization Factor in Response Assessment of the Mistuned Bladed Disk

In this section, the influences of random mistuning and the intentional mistuning on the amplitude magnification will be discussed, and their mechanisms will also be explained using the concepts of NDS and MEF. The amplitude magnification factor $\beta$ is defined as

$$\beta = \frac{U_m}{U_n} \tag{13}$$

where $U_m$ and $U_n$ are the maximal response amplitudes in a frequency range of the mistuned and the tuned bladed disks.

Here, we consider two kinds of EO excitation: $E = 9$ and $E = 14$. For the tuned bladed disk, the former can excite the modes in the veering region, and the latter can excite two sets of modes with well-separated natural frequencies.

### A. Random Mistuning and Threshold Phenomenon

Using the same random mistuning samples in Sec. III.D, the mean of the calculated MEFs of a randomly mistuned blade disk are shown in Fig. 7. In this section, we will give comprehensive explanations of the threshold phenomenon using the concepts of MEF and MLF.

For $E = 14$, if the bladed disk is tuned, there will be two pairs of modes with 14 nodal diameters to be excited by the given excitation, and they are the 28th, 29th, 84th, and 85th modes, respectively. The first pair of modes is blade dominated, and the second pair is disk dominated. The mean values of the MLFs and MEFs when the bladed disk is mistuned are listed in Table 1. The results indicate that the modes shapes of the first pair change greatly and are highly localized, while the modes of the second pair change sightly, and their MLFs are very small. For the MEFs, there is only one peak at the disk-dominated modes, and their values are close to one. For the blade-dominated modes, although the modes are localized, the modal excitations are small; for the disk-dominated modes, which are not sensitive to blade mistuning, the large MEFs would not lead to localized vibration. Therefore, there would be no severe amplitude magnification phenomenon induced by $E = 14$.

When $E = 9$, the MEFs have two obvious peaks, even for the mistuned cases: one corresponds to the blade–disk coupled vibration modes (the 18th and 19th orders) and the other to the disk-dominated modes (the 74th and 75th orders). The results of the MLFs and MEFs are listed in Table 2, and the amplitude magnification factors are shown in Fig. 8. The second peak of the MEFs is much like the peak for $E = 14$, and it would not cause large vibration amplitudes of the blades. For the first peak, when the mistuning strength is small ($dk = 0.01$), the mode localization is acceptable, but the MEFs are considerable large; therefore, the mean response amplitude factors are up to 1.5, even with the small mistuning.

With the increase of mistuning strength, since the excited mistuned modes deviate from the tuned modes, the MLFs increase and the MEFs decrease monotonically. The MEF determines the ability to receive the excitation energy, and the MLF determines whether the excited modes are highly localized. Therefore, there should be a peak value for the medium strength of random mistuning, and we refer to it as the threshold phenomenon. When the strength of

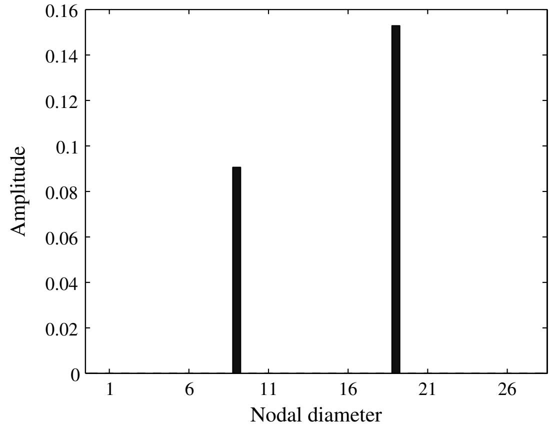

**Fig. 12 NDS of 46th mode with $h$28 intentional mistuning.**

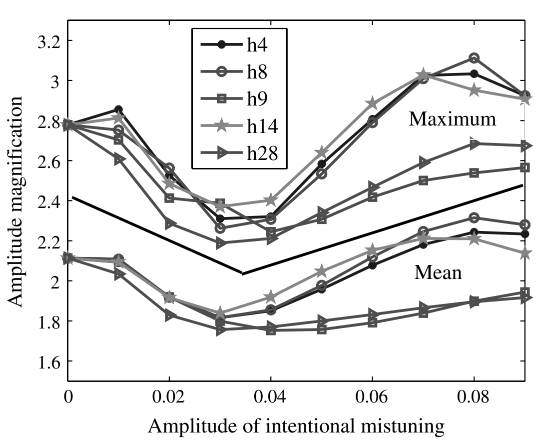


**Fig. 13 Amplitude magnification with random and intentional mistunings.**

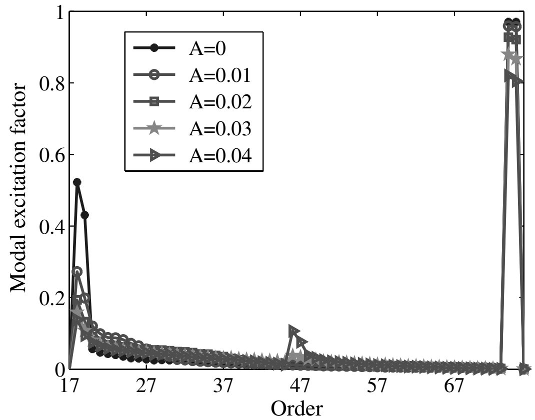


**a) *A*=0–0.04**

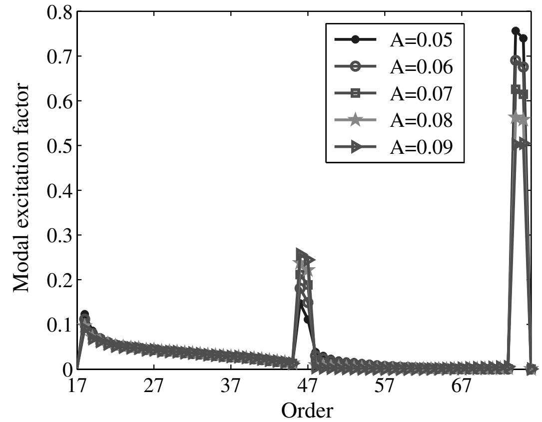


**b) *A*=0.05–0.09**

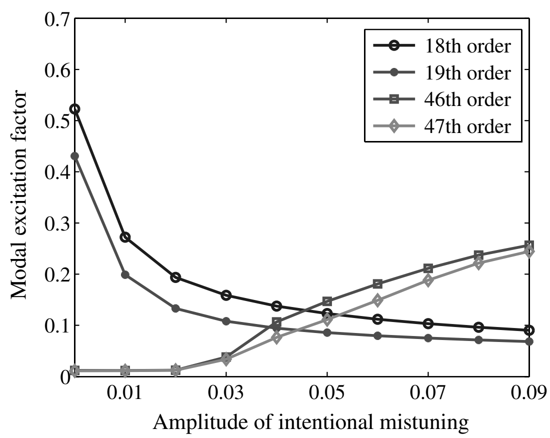


**c) MEFs of 18th, 19th, 46th, and 47th order**

**Fig. 14 MEFs with *h*28 intentional mistunings.**

random mistuning is smaller than the threshold value, the increase of the MLFs is the dominant reason for the increase of the amplitude magnification factors, and when it is larger than the threshold value, the decrease of the MEFs becomes the dominant reason for the decrease of the amplitude magnification factors.

### B. Effects of Intentional Mistuning

Here, we consider the intentional mistuning in harmonic form,

$$\Delta k_{1i} = A \sin\left(\frac{h(i-1)}{N} 2\pi\right) \tag{14}$$

where $\Delta k_{1i}$ is the intentional stiffness change of the $i$th blade, $A$ is the amplitude, and $h$ is the harmonic integer of intentional mistuning.

The amplitude magnification factors of a bladed disk with intentional mistuning are shown in Fig. 9. We also note that these two kinds of intentional mistuning also exhibit the threshold phenomenon with the amplitude of intentional mistuning and can be explained by the combined effects of the MLF and MEF. The results indicate that the $h28$ intentional mistuning has the smallest amplitude magnification, since this type of intentional mistuning keeps the cyclic symmetry property of the structure and does not lead to severe mode localization. We also note that the amplitude magnification factors with $h9$ intentional mistuning vary in the same way as the ones with $h28$ type, but the values are much larger, since this kind of intentional mistuning destroys the symmetry property much more. In practice, we always prefer the type that can be implemented more easily. For the given example of a bladed disk, $h28$ intentional mistuning is preferred, because it only needs two kinds of blade stiffness.

The NDS of the 18th mode with different types of intentional mistuning is shown in Fig. 10. We can see that the new nodal diameter component (19 nodal diameter) emerges after adding $h28$ intentional mistuning to the tuned bladed disk, and the original nine-nodal-diameter content decreases. Figure 11a shows the MEFs with $h28$ intentional mistuning. Compared with the bladed disk without intentional mistuning, the MEFs at the 18th and 19th orders become smaller, but a new peak emerges at the 46th and 47th orders. The reason is that, after the intentional mistuning is introduced, the 18th and 46th modes both consist of the 9 nodal and 19 nodal diameters, as shown in Fig. 12. Similarly, new nodal diameter components and peaks of the MEFs emerge when the $h9$ intentional mistuning is added to the bladed disk, as shown in Figs. 10b and 11b.

### C. Combined Effects of Random and Intentional Mistuning

In this section, the effects of both random and intentional mistuning are considered to validate whether the adverse influence of random mistuning is suppressed. According to the results in Sec. IV.A, the mistuning strength [−0.03, 0.03] can lead to the maximum amplitude magnification. Therefore, we take this set of random mistuning as the research object and investigate the effects of different kinds of intentional mistunings.

The mean and maximal values of amplitude magnification factors obtained from a Monte Carlo simulation of the example of the bladed disk with random and intentional mistuning is shown in Fig. 13. For the traveling wave excitation with $E = 9$, both the $h28$ and $h9$ intentional mistunings can effectively alleviate the unfavorable amplitude magnification. Nevertheless, the mechanisms of the two kinds of intentional mistunings are slightly different, since $h28$ keeps the cyclic symmetry property and $h9$ destroys it drastically, as discussed in Sec. IV.C.

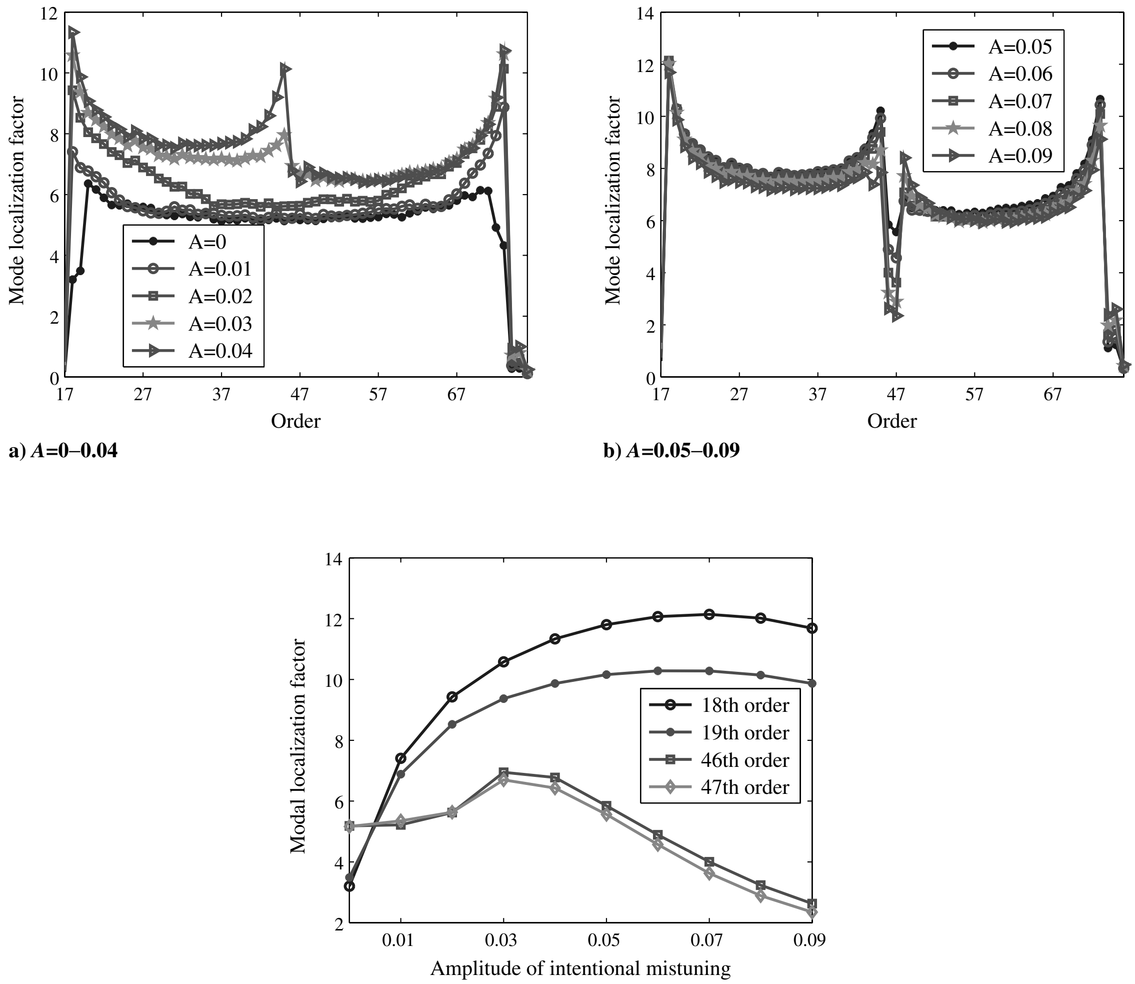


**a) $A$=0–0.04**

**b) $A$=0.05–0.09**

**c) MLFs of 18th, 19th, 46th, and 47th order**

**Fig. 15 MLFs with $h$28 intentional mistunings.**

*1. h28 Intentional Mistuning*

The MEFs with $h$28 intentional mistuning are shown in Fig. 14. There are two peaks at the 18th and 19th orders and the 46th and 47th orders in the blade-dominated modes family. With the increase of the intentional mistuning amplitude $A$, the values of the first peak first decrease rapidly and then remain around 0.1, while the second peak first remains unchanged around 0.01 and then increases, as shown in Fig. 14c.

The MLFs with intentional mistuning are shown in Fig. 15. It can be seen that, with the increase of $A$, the MLFs of the 18th and 19th modes first increase rapidly and then keep the value around 12 and 10, respectively. While the MLFs of the 46th and 47th modes first increase very slowly and then decrease.

According to the preceding results, we can conclude the following:

1) The variation of amplitude magnification of the bladed disk with random and intentional mistunings is also the results of the combined influences of MEF and MLF at the two peak positions of the MEFs.

2) When $A$ is smaller than 0.03–0.04, the decrease of the MEFs at the 18th and 19th modes is the main reason for the decrease of amplitude magnification.

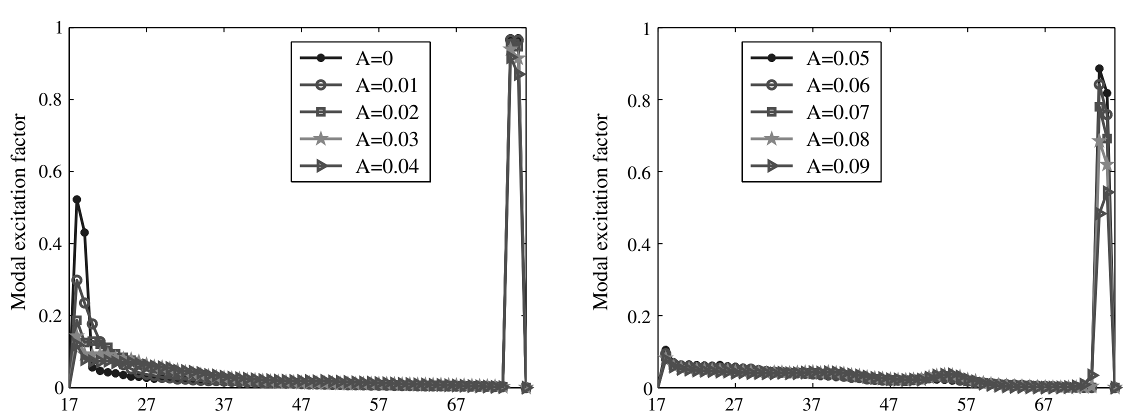


**a) $A$=0–%4**

**b) $A$=%5–%9**

**Fig. 16 MEFs with $h$9 intentional mistunings.**

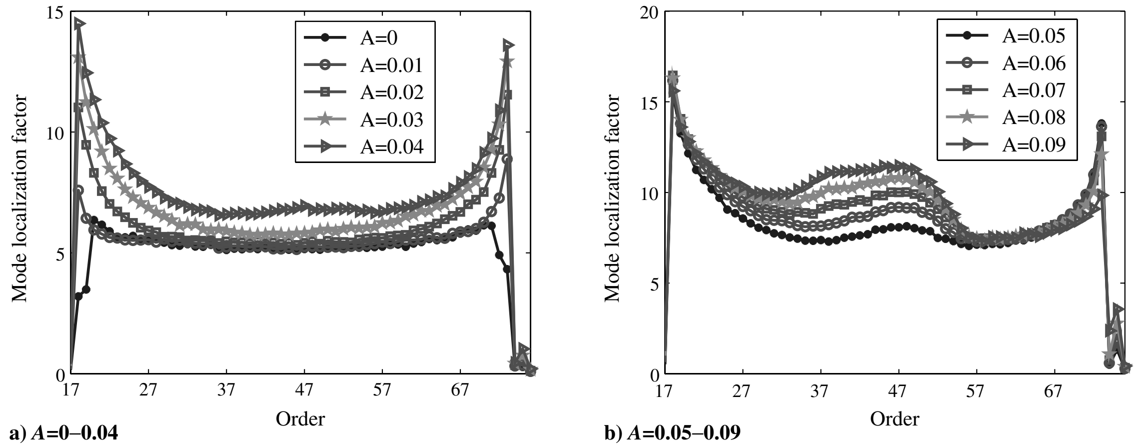


**Fig. 17 MLFs with $h9$ intentional mistunings.**

3) When $A$ is greater than 0.04, the MEFs and MLFs of the 18th and 19th modes almost remain unchanged. Although the MLFs decrease with the increase of intentional mistuning amplitude, the rise of the MEFs becomes the dominant factor and makes the amplitude magnification increase gently.

*2. h9 Intentional Mistuning*

It can be seen in Fig. 16 that the MEFs of the bladed disk with $h9$ intentional mistuning have only one peak in the blade-dominant modes family. And with the increase of $A$, the values of the peak first decrease rapidly and then keep decreasing slowly around 0.1, varying in the same way as the $h28$ mistuning type. Figure 17 shows the MLFs with $h9$ intentional mistuning. It is noted that, when $A > 0.04$, the MLFs of the 25th–54th modes increase with the increase of $A$.

The main difference in the $h28$ intentional mistuning lies in that, because the given $h9$ type totally destroys the cyclic symmetry property of the bladed disk, no new MEF peaks emerge; therefore, the increasing MLFs become the dominant factors of the gentle increase of amplitude magnification when $A > 0.04$, in Fig. 13.

As a final remark, for the bladed disk with random mistuning, the introduced intentional mistuning spreads out the nodal diameter components of the random mistuned modes and makes the rotor less susceptible to being strongly excited by the given EO excitation. Simply put, the intentional mistuning makes the modal excitation smaller by changing the mistuned modes. It should be noted that the introduced intentional mistuning also changes the MLFs of the bladed disks. The reason for the increase of amplitude magnification when $A$ is greater than the optimal value is either the new increasing peaks of modal excitation ($h28$ intentional mistuning) or the more localized blade-dominant modes caused ($h9$ intentional mistuning) by intentional mistuning, or even their combinations.

## V. Conclusions

The application of the NDS of mode shapes in the assessment of dynamic characteristics for a bladed disk has been proposed in this paper.

For the free vibration, we improve the definition of the MLF using NDS. The improved MLF based on the maximal modal displacement is simple, has more clear physical meaning, and can be used as an effective measure for the localization level of the mistuned modes.

For the forced vibration, the MEF is defined to give an estimation of the capability of the mistuned modes for receiving energy from the EO excitation. The threshold phenomenon of amplitude magnification in a randomly mistuned bladed disk and the benefit of intentional mistuning can be well explained using the MEF and the MLF. The results indicate that the amplitude magnification is determined by the MEFs under the given EO excitation and the mode localization level of the reached modes. The key mechanism of intentional mistuning lies in that it makes the MEFs much smaller by spreading out the nodal diameter contents of the mistuned modes and by changing the extent of mode localization. With the increase of harmonic intentional mistuning amplitude $A$, due to the new emerging peaks of MEFs in blade-dominant modes, more localized modes, or their combinations, the amplitude magnification of the random mistuned bladed disk will increase again when $A$ is greater than the optimal value.

The increase of random mistuning strength or introduced intentional mistuning is not only changing the MEFs (or, say, spreading out the NDS of mistuned modes), it also changes the MLFs of the mistuned modes. With different mistuning conditions, either the MEFs or MLFs could be the dominant reason for the changes of the magnification factors.

## References


[1] Wang, J. J., Li, Q. H., and Zhu, Z. G., "Vibratory Localization of Mistuned Bladed Disk Assemblies: A Review," *Advances in Mechanics*, Vol. 30, No. 4, 2000, pp. 517–528.

[2] Castanier, M. P., and Pierre, C., "Modeling and Analysis of Mistuned Bladed Disk Vibration: Status and Emerging Directions," *Journal of Propulsion and Power*, Vol. 22, No. 2, 2006, pp. 384–396. doi:10.2514/1.16345

[3] Wang, J. J., Yao, J. Y., and Li, Q. H., "Probability Characteristics of Vibratory Mode of Bladed Disk Assemblies with Random Stiffness Mistuning," *Journal of Aerospace Power*, Vol. 23, No. 2, 2008, pp. 256–262.

[4] Wang, J. J., Yu, C. B., Yao, J. Y., and Li, Q. H., "Vibratory Mode Localization Factors of Mistuned Bladed Disk Assemblies," *Journal of Propulsion Technology*, Vol. 30, No. 4, 2009, pp. 457–461.

[5] Castanier, M. P., and Pierre, C., "Using Intentional Mistuning in the Design of Turbomachinery Rotors," *AIAA Journal*, Vol. 40, No. 10, 2002, pp. 2077–2086. doi:10.2514/2.1542

[6] Klauke, T., Kühhorn, A., Beirow, B., and Golze, M., "Numerical Investigations of Localized Vibrations of Mistuned Blade Integrated Disks (Blisks)," *Journal of Turbomachinery*, Vol. 131, No. 3, 2009, Paper 031002. doi:10.1115/1.2985074

[7] Castanier, M. P., and Pierre, C., "Investigation of the Combined Effects of Intentional And Random Mistuning on the Forced Response Of Bladed Disks," AIAA Paper 1998-3720, 1998.

[8] Choi, B.-K., Lentz, J., Rivas-Guerra, A. J., and Mignolet, M. P., "Optimization of Intentional Mistuning Patterns for the Reduction of the Forced Response Effects of Unintentional Mistuning: Formulation and Assessment," *Journal of Engineering for Gas Turbines and Power*, Vol. 125, No. 1, 2003, pp. 131–140. doi:10.1115/1.1498270

[9] Yao, J. Y., Wang, J. J., and Li, Q. H., "Robustness Analysis of Mistuned Bladed Disk Using the Upper Bound of Structured Singular Value," *Journal of Engineering for Gas Turbines and Power*, Vol. 131, No. 3, 2009, Paper 032501. doi:10.1115/1.3018942

[10] Ottarsson, G., and Pierre, C., "On the Effects of Interblade Coupling on the Statistics of Maximum Forced Response Amplitudes in Mistuned

Bladed Disks," AIAA Paper 1995-1494, 1995.
[11] Yang, M.-T., and Griffin, J. H., "A Reduced-Order Model of Mistuning Using a Subset Of Nominal System Modes," *Journal of Engineering for Gas Turbines and Power*, Vol. 123, No. 4, 2001, pp. 893–900. doi:10.1115/1.1385197
[12] Feiner, D. M., and Griffin, J. H., "A Fundamental Model of Mistuning for a Single Family of Modes," *Journal of Turbomachinery*, Vol. 124, No. 4, 2002, pp. 597–605. doi:10.1115/1.1508384
[13] Rotea, M., and D'Amato, F., "New Tools for Analysis and Optimization of Mistuned Bladed Disks," AIAA Paper 2002-4081, 2002.
[14] Whitehead, D. S., "Effect of Mistuning on the Vibration of Turbo-Machine Blades Induced by Wakes," *Journal of Mechanical Engineering Science*, Vol. 8, No. 1, 1966, pp. 15–21. doi:10.1243/JMES_JOUR_1966_008_004_02

R. Miller
*Associate Editor*